Front. Med. 2019, 13(5): 575–589
https://doi.org/10.1007/s11684-019-0693-9

RESEARCH ARTICLE

Glycosylation of dentin matrix protein 1 is critical for fracture healing via promoting chondrogenesis

Hui Xue[1,*], Dike Tao[1,*], Yuteng Weng[1], Qiqi Fan[1], Shuang Zhou[1], Ruilin Zhang[1], Han Zhang[2], Rui Yue[3], Xiaogang Wang (✉)[4], Zuolin Wang (✉)[1], Yao Sun (✉)[1]

[1]Department of Implantology, School & Hospital of Stomatology, Tongji University, Shanghai Engineering Research Center of Tooth Restoration and Regeneration, Shanghai 200072, China; [2]School & Hospital of Stomatology, Tongji University, Shanghai 200072, China; [3]School of Life Sciences and Technology, Tongji University, Shanghai 200072, China; [4]Beijing Advanced Innovation Center for Big Data-Based Precision Medicine, Beihang University, Beijing 100083, China

Abstract **Fractures are frequently occurring diseases that endanger human health. Crucial to fracture healing is cartilage formation, which provides a bone-regeneration environment. Cartilage consists of both chondrocytes and extracellular matrix (ECM). The ECM of cartilage includes collagens and various types of proteoglycans (PGs), which play important roles in maintaining primary stability in fracture healing. The PG form of dentin matrix protein 1 (DMP1-PG) is involved in maintaining the health of articular cartilage and bone. Our previous data have shown that DMP1-PG is richly expressed in the cartilaginous calluses of fracture sites. However, the possible significant role of DMP1-PG in chondrogenesis and fracture healing is unknown. To further detect the potential role of DMP1-PG in fracture repair, we established a mouse fracture model by using a glycosylation site mutant DMP1 mouse (S89G-DMP1 mouse). Upon inspection, fewer cartilaginous calluses and down-regulated expression levels of chondrogenesis genes were observed in the fracture sites of S89G-DMP1 mice. Given the deficiency of DMP1-PG, the impaired IL-6/JAK/STAT signaling pathway was observed to affect the chondrogenesis of fracture healing. Overall, these results suggest that DMP1-PG is an indispensable proteoglycan in chondrogenesis during fracture healing.**

Keywords fracture; extracellular matrix; dentin matrix protein 1; proteoglycan; cartilage

Introduction

Fracture healing is a complex and sequential process consisting of four overlapping phases: activated inflammation, cartilaginous callus formation, hard callus formation, and callus remodeling [1,2]. The initial phase of bone repair is hematoma formation, followed by inflammation cascades [3,4]. Inflammatory cells enter into the fibrin network of hematoma and release cytokines into fracture sites [5]. Under the stimulation of cytokines, mesenchymal stem cells (MSCs) differentiate into chondrocytes undergoing hypertrophy and secreting cartilage matrix, which is finally replaced by cortical bone to support mechanical loading [1,2]. Thus, cartilage formation is critical in fracture healing.

The cartilage consists of chondrocytes and extracellular matrix (ECM), including types II and X collagens and proteoglycans (PGs) [6]. PGs are composed of small core proteins and relatively large glycosaminoglycan chains that are connected to core proteins through the covalent bonds [7]. Although the percentage of PGs in the cartilage matrix is less than 5%, PGs play a critical role in maintaining cartilage properties by maintaining mechanical strength [8]. PGs also possess functions, such as maintaining the durability of mineralized matrix, filling extracellular space, maintaining tissue hydration, storing growth factors and enzymes, maintaining organizational flexibility, providing protective barriers, and mediating the activities of secreted proteins [9–11]. The breakdown of PGs is closely associated with cartilage degeneration, osteoarthritis development, and fracture healing [12–14].

Received September 17, 2018; accepted February 25, 2019
Correspondence: Yao Sun, yaosun@tongji.edu.cn;
Zuolin Wang, zuolin@tongji.edu.cn;
Xiaogang Wang, xiaogangwang@buaa.edu.cn

*These authors contributed equally to this work.

Dentin matrix protein 1 (DMP1) is an acid non-collagen ECM protein first found in odontoblasts and highly expressed in the bone matrix [15,16]. After posttranslational modification, the full-length form of DMP1 protein can be processed into two terminal fragments, namely, the N- and C-terminal fragments [17,18]. DMP1 C-terminal fragment, which is highly phosphorylated, is closely involved in bone mineralization [19,20]. Interestingly, the DMP1 N-terminal can be modified into a form of glycosylation, named the PG form of dentin matrix protein 1 (DMP1-PG), which is also a key molecule in osteogenesis. In addition to the expression of DMP1-PG in the mineralization matrix, it is highly expressed in the cartilage matrix, and its loss can accelerate the destruction of articular cartilage in the temporal–mandibular joint [9,21,22]. Importantly, the serine^{89} of bone and cartilage matrix is a highly conserved glycosylated amino acid site and is the only glycosylation site of DMP1-PG in mice [7,23,24].

Chondrogenesis is one of the major steps of fracture healing [25]. DMP1-PG is a newly identified PG, which is a key molecule in chondrogenesis [9]. In the current study, we found that DMP1-PG was highly expressed in the cartilage matrix of fracture callus. We further compared the expression levels of several types of PGs during fracture healing. The increased *Dmp1* was the largest observed, and the expression level of *Dmp1* was continuously upregulated at days 7 and 21 post-operation. Thus, we hypothesized that DMP1-PG may play an essential role in chondrogenesis during bone fracture repair. By using a genetically modified DMP1 mouse (S89G-DMP1 mouse), we set up a stable femur fracture model to verify the critical role of DMP1-PG within the process of fracture healing. The role of DMP1-PG in modulating the formation of cartilaginous calluses was systematically analyzed during the fracture healing. Using data from RNA sequencing and related techniques, we investigated the potential mechanism of DMP1-PG in regulating cartilaginous callus formation.

Materials and methods

Animals

The generation of S89G-DMP1 mice is described in a recent study [7]. In brief, the gene knock-in technique was adopted to substitute the serine^{89} of DMP1 with glycine to interfere with the normal glycosylation of DMP1-PG. All of the experimental animals were raised in the SPF facility under a 12-h light/dark cycle. All of the experimental protocols performed on the mice were approved by the Animal Welfare Committee of Tongji University (TJLAC-017-027).

Fracture model

An established fracture model was generated as previously described [26]. In brief, 3-month-old male wild-type (WT) mice, 3-month-old male S89G-DMP1 mice, and 12-month-old male WT mice were employed to establish the fracture models. After anesthesia induction with isoflurane inhalation, the skin of surgical area was disinfected, and a 2 cm skin incision was made along the anterolateral shaved femur. A 24-gauge sterile needle was inserted into the medullary canal through the femur plateau, and the syringe needle was partially removed. A no. 11 surgical blade was used to transect the middle diaphysis of the femur, and the fracture site was stabilized by re-inserting the syringe. The periosteum adjacent to the fracture site was protected carefully to avoid human intervention. After washing with 0.9% normal saline carefully, a 4-0 silk suture was used to close the muscle flap and skin. Buprenorphine was used as analgesic via intraperitoneal injection for 3 d post-fracture.

Micro-computed tomography (CT) analysis

The 3-month-old WT mice and 3-month-old S89G-DMP1 mice were sacrificed at indicated time points post-fracture (5 mice per group per time point), and the femur fracture specimens were fixed in 4% paraformaldehyde overnight at 4 °C. A Scanco micro-CT 50 instrument at a scan resolution of 10 μm was used to perform radiological imaging analysis with a voltage of 70 kV and a current of 200 μA. The calluses of specimens were scanned and analyzed at 1 mm distal and 1 mm proximal from the fracture ends [27]. The parameters of callus bone volume/total volume, bone mineral density (BMD), trabecular number, trabecular thickness, and trabecular space were quantified according to the standard procedures.

Biomechanical testing

A three-point bending test was performed to examine the new bone mechanical properties of fractured femurs. In brief, at 4 weeks post-operation, the femur fracture samples (5 mice per group) isolated from the 3-month-old WT mice and 3-month-old S89G-DMP1 mice were tested to failure by using a biomechanical testing machine (Farui Co., China). Loading force in testing was exerted at a rate of 10 mm/min until failure. The maximum displacement (mm) and maximum bending load (N) were determined and analyzed from bending force–deflection curves.

Histology, immunohistochemistry, and immunofluorescence

After fixation in paraformaldehyde and removal of the surgical pins, the isolated femur fracture specimens were

demineralized in 10% EDTA for 3 weeks at 4 °C. The muscle and surrounding soft tissues were not removed completely to preserve the basic callus structures around the fracture sites. The samples were then embedded into paraffin and cut into 5 μm sections. Histological staining, including hematoxylin and eosin (H&E), Toluidine blue, and Safranin O staining, was conducted. Safranin O staining was applied to detect and calculate an interesting area of the fracture callus. For immunohistochemistry staining, the following primary antibodies were used to observe the protein expression of the cartilage matrix: anti-collagen II (COL-II, 1:200; Boster), anti-collagen X (COL-X, 1:200; Boster), anti-SOX9 (1:200; Boster), anti-aggrecan (ACAN, 1:100; Boster), anti-decorin (DCN, 1:100; Boster), anti-versican (VCAN, 1:100; Boster), and anti-DMP1-N-9B6.3 (1:500; gift from Dr. Chunlin Qin, Baylor College of Dentistry). Protein expression was detected by a DAB detection kit. The areas of positive staining zones (COL-II, COL-X, ACAN, DCN, and VCAN), number of positive cells (SOX 9), total callus areas, and number of total cells in the callus were analyzed using the ImageJ software (NIH, Bethesda, MD, USA). The positive area/total callus area or the number of positive cells/the number of total cells were used to compare the immunohistochemistry difference between WT mice and S89G-DMP1 mice, and detailed semiquantitative methods have been described [9]. The sections for immunofluorescence were incubated with IL-6 antibody (1:300; Abcam) at 4 °C overnight and then incubated with Alexa Fluor 488 IgG (1:800; Invitrogen) for 1 h at room temperature. Finally, DAPI was applied to counterstain the sections.

Bone marrow MSC (BMSCs) isolation and culture

BMSCs were isolated from the medullary cavities of 4-week-old WT mice and S89G-DMP1 mice (12 mice per group). In brief, after anesthesia induction, the mice femurs and tibias were separated carefully and cut at both ends. The bone marrows were then aseptically rinsed into petri dishes. The marrow tissues were cultured with growth media consisting of α-MEM, 10% FBS (Excell) and 1% penicillin/streptomycin (Gibco). BMSCs were cultured in osteoblastic (Gibco) and chondrogenic (Gibco) medium for 21 d. For chondrogenesis induction, BMSCs were cured in micromass culture system as previously reported [28]. The cells were then stained with Alizarin red and Toluidine blue to observe the culture aggregates. Cell Counting Kit-8 Assay (Dojindo) was performed in accordance with the manufacture's protocols to evaluate the proliferative ability of the BMSC. Cell proliferation was measured at days 1, 3, 5, and 7. For Transwell migration assay, 1×10^4 BMSCs were seeded in the upper chamber with 100 μL of serum-free medium. The lower chamber was filled with 700 μL of medium containing 10% FBS. Crystal violet and DAPI staining were performed after 12 h of incubation.

Real-time quantitative polymerase chain reaction

The calluses, including 4 mm bony segments from 3-month-old WT mice and 3-month-old S89G-DMP1 mice fracture sites were isolated carefully at days 1, 3, 7, 14, and 21 post-fracture (4–6 mice per group per time point) and then placed into liquid nitrogen immediately for homogenization. The homogenized samples and chondrogenic or osteogenic cultured BMSCs were added with TRIzol reagent (Invitrogen). Total RNA was extracted and reverse-transcribed into cDNA at a volume of 20 μL of a commercial kit (Roche). The expression of the target gene was observed and detected using a Light Cycler 96 PCR system (Roche). The reactions of each sample needed to be run in triplicate. The gene-specific primers are listed in Table S1.

RNA sequencing and data analysis

Total RNA was extracted from the fracture calluses of 3-month-old WT and 3-month-old S89G-DMP1 group at day 3 post-fracture (5 mice per group). A Nano Vue (GE) was used to assess RNA purity, and an Agilent 2200 Tape Station (Agilent Technologies) was employed to evaluate RNA integrity. RNA sequencing was performed at Novogene Co., Ltd., Beijing. The detailed protocol was similar to that described previously [29]. All differentially expressed genes were collected for the heat map. Kyoto Encyclopedia of Genes and Genomes (KEGG) enrichment analysis was performed to detect the changed signaling pathway, and a threshold of Q-value of < 0.05 was used to determine significant enrichment of gene sets.

Western immunoblotting

Total proteins were harvested from the fracture calluses of femurs of WT mice and S89G-DMP1 mice at day 1 (3-month-old WT mice, $n = 3$; 3-month-old S89G-DMP1 mice, $n = 3$), day 3 (3-month-old WT mice, $n = 3$; 3-month-old S89G-DMP1 mice, $n = 3$) and day 7 (3-month-old WT mice, $n = 3$; 3-month-old S89G-DMP1 mice, $n = 3$; 12-month-old WT mice, $n = 3$) post-fracture. BCA protein assay kit was used to determine protein concentration after extraction. The expression levels of DMP1-PG, signal transducers, activators of transcription 3 (STAT-3), and P-STAT-3 were detected, and the following monoclonal antibodies were employed at different dilutions: anti-DMP1-N-9B6.3 (1:1500; gift from Dr. Chunlin Qin, Baylor College of Dentistry), anti-STAT3 (1:500; Boster), and anti-P-STAT3 (1:500; Boster). Anti-β-actin antibodies were used to probe each sample.

Statistical analysis

Student's *t* test for comparing the difference between two groups was performed using the GraphPad Prism 7.00 software. For the comparison of three groups, two-way ANOVA was applied. Results were deemed statistically significant at P values < 0.05, and all values were presented as mean ± SEM.

Results

DMP1-PG expression during fracture healing

To observe the expression of DMP1-PG in cartilaginous callus, we set up a femur fracture model in WT mice. The Toluidine blue staining (i.e., a specific blue staining for proteoglycan molecules in tissue) indicated that the PGs were involved in fracture repair (Fig. 1A). Compared with the 3-month-old WT mice, the 12-month-old WT mice showed less cartilaginous callus and more fibrous callus in their fracture sites (Fig. 1B). During fracture healing, the gene expression levels of PGs that correlated with chondrogenesis were evaluated. Among the significantly upregulated PGs, *Dmp1* was continuously increased at both days 7 and 21 post-fracture. Except for *Dmp1*, other PG molecules showed downregulated expression at day 21 post-fracture (Fig. 1C). Immunohistochemistry staining was performed to observe the expression of DMP1-full-length (DMP1-F)/DMP1-PG by using an anti DMP1-N-terminal antibody, and the DMP1-F/DMP1-PG was extensively expressed in cartilaginous calluses at day 7 post-operation (Fig. 1D). Western immunoblotting confirmed that DMP1-PG in femur callus samples was rich in 3 months and downregulated in 12 months (Fig. 1E).

Impaired chondrogenesis and fracture healing in S89G-DMP1 mice

To further investigate the role of DMP1-PG in fracture healing, we employed a DMP1 point mutation mice called S89G-DMP1 mice, where S^{89} is the only glycosylation site in mice (Fig. 2A). Western immunoblotting showed significantly downregulated DMP1-PG expression in the protein extracts from fracture calluses of the S89G-DMP1 femurs compared with WT controls at day 7 post-fracture (Fig. 2B). To monitor the fracture healing of femurs in S89G-DMP1 and WT mice, we performed micro-CT scanning to compare the differences of callus formation. A decreased total volume of mineralized calluses and increased numbers of porous new bones were detected in the fracture areas of S89G-DMP1 mice at both days 14 and 21 post-fracture. At day 28 post-fracture, partial fracture gaps can still be observed on the specimens of S89G-DMP1 mice, which was caused by blocking the PG of DMP1 (Fig. 2C). Compared with WT mice, micro-CT quantification assessment displayed abnormal changes in fracture callus in the S89G-DMP1 mice (Fig. 2D). Biomechanical testing, a definitive measure of fracture repair [30], was employed on the fractured femurs of WT and S89G-DMP1 mice to examine the mechanical property of the new bone at day 28 post-fracture when the bony callus has matured. Three-point bending tests displayed a marked decrease of bending resistance ability in the S89G-DMP1 mice compared with the control group (Fig. 2E).

H&E, Toluidine blue, and Safranin O staining were conducted to evaluate callus formation at days 7, 14, 21, and 28 post-fracture. At day 7, cartilage areas were significantly decreased in S89G-DMP1 mice, suggesting an impairment of chondrogenesis (Fig. 3A). At day 14 after fracture, a large callus, including cartilaginous callus and osseous callus, can be observed in WT mice. Compared with the control groups, the callus in S89G-DMP1 mice displayed lesser cartilage and deposited new bone areas (Fig. 3A). At day 21 post-fracture, most of the cartilaginous calluses were replaced by the woven bone in both S89G-DMP1 and WT mice. The areas of bony callus in the S89G-DMP1 mice were much smaller than those of the WT controls. The cortical bone continuity remained poor in the S89G-DMP1 mice (Fig. 3A). After 4 weeks, compared with the WT controls, the S89G-DMP1 mice showed significantly smaller areas of new bone bridging the fracture sites (Fig. 3A). Histomorphometric measurements of cartilaginous and osseous callus at days 7, 14, 21, and 28 post-fracture showed significantly decreased cartilage and new bone areas in the S89G-DMP1 group (Fig. 3B and 3C).

Molecular changes of cartilaginous calluses between WT and S89G-DMP1 mice

To further analyze the effects of DMP1-PG on cartilaginous callus formation, the expression levels of cartilage markers, such as collagen II, collagen X, SOX9, aggrecan, decorin, and versican, were evaluated by immunohistochemistry staining (Fig. 4A1–4A6, 4B1–4B6, 4C1–4C6). The decreased expression levels of cartilage markers were observed in cartilaginous calluses of S89G-DMP1 mice at day 7 post-fracture. In addition to the immunohistochemistry staining, RT-qPCR was performed to determine the expression levels of chondrogenic markers. Lower expression levels of marker genes were evident in S89G-DMP1 mice compared with controls at days 7 and 14 post-fracture but were not yet apparent at day 21 post-fracture due to the shift from cartilage to woven bone (Fig. 4D1–4D6). Collectively, our data demonstrated a positive effect of DMP1-PG in regulating chondrogenesis during fracture repair.

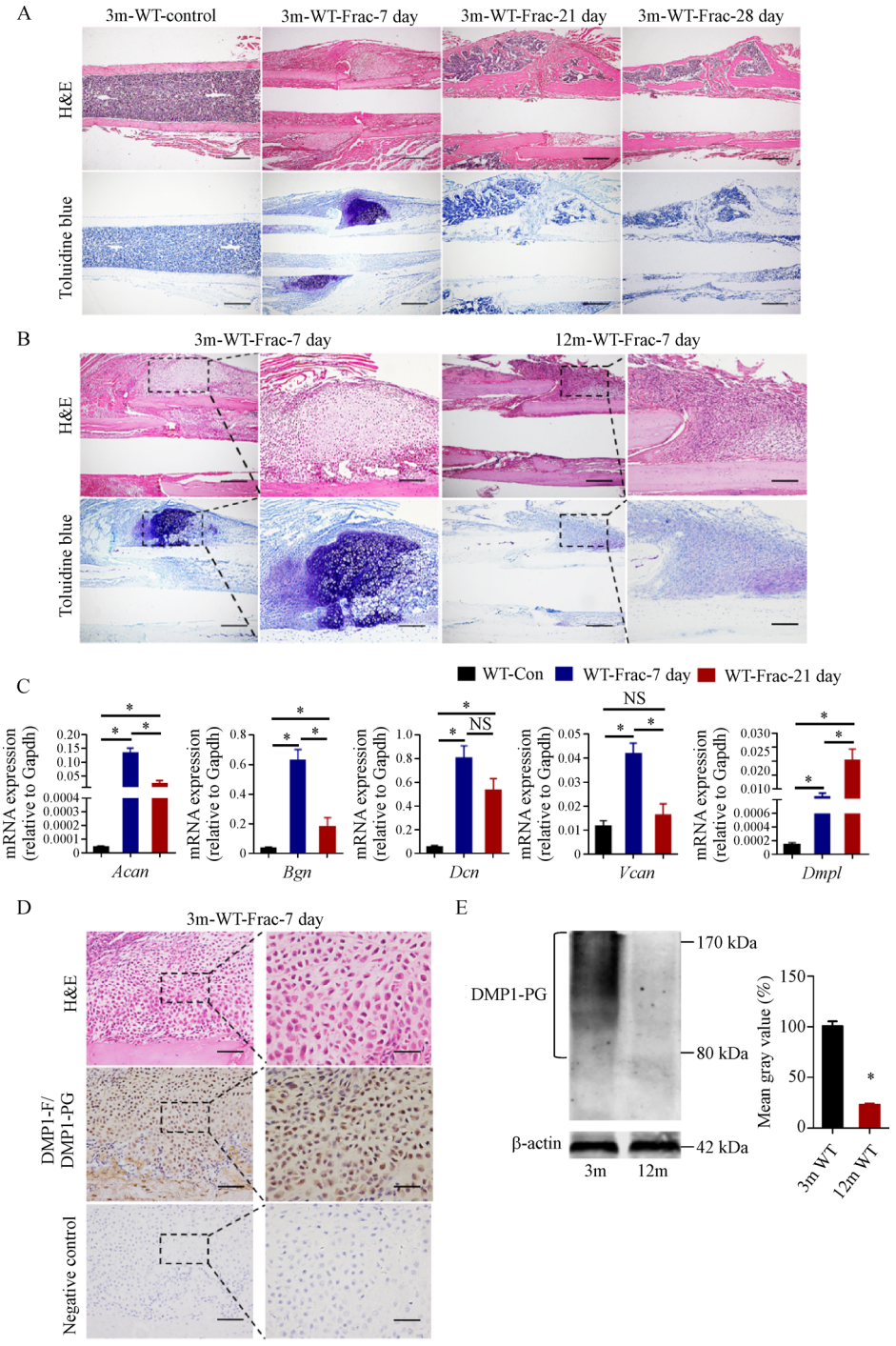

Fig. 1 Expression of DMP1-PG in cartilage callus during fracture healing. (A) H&E and Toluidine blue staining of unfractured femurs and fractured femurs is shown at days 7, 21, and 28 post-fracture in WT mice. Scale bars = 500 μm. (B) Weaker cartilaginous calluses were formed in the 12-month-old WT mice compared with those of the 3-month-old WT mice at day 7 post-fracture. Lower magnification, scale bars = 500 μm; higher magnification, scale bars = 200 μm. (C) RT-qPCR quantification of *Acan, Bgn, Dcn, Vcan,* and *Dmp1* in the fracture calluses from normal mice and fracture model mice. Data are shown as mean ± SEM. $*P < 0.05$, $n = 3$ per time point. NS, not significant. (D) DMP1-F/DMP1-PG was expressed in the cartilaginous calluses of the fracture model mice. Lower magnification, scale bars = 100 μm; higher magnification, scale bars = 50 μm. (E) The expression level of DMP1-PG was downregulated in the fracture callus of the 12-month-old WT mice compared that of the 3-month-old WT mice at day 7 post-operation by Western immunoblotting. $*P < 0.05$, $n = 3$ per group. 3m, 3-month-old; 12m, 12-month-old.

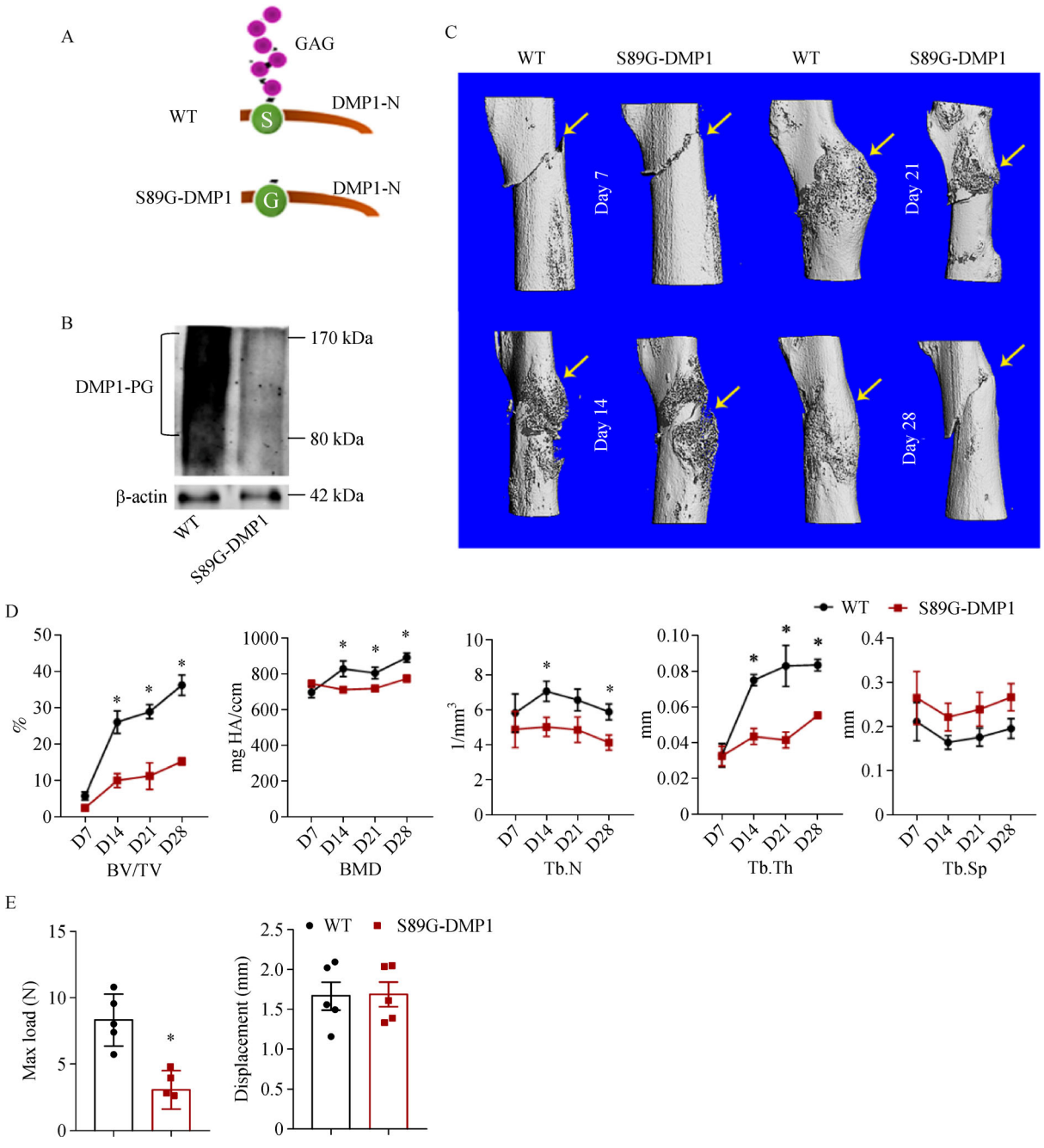

Fig. 2 Delayed femur fracture healing in S89G-DMP1 mice. (A) A schematic of the DMP1-PG point mutation model is shown. (B) Decreased DMP1-PG expression in the fracture callus of the S89G-DMP1 mice is shown at day 7 post-fracture by Western immunoblotting. (C) Representative three-dimensional reconstruction of micro-CT images of fracture sites at days 7, 14, 21, and 28 post-fracture. Arrows show the fracture gaps and calluses. (D) The quantitative micro-CT analysis of fracture callus is shown as mean ± SEM. *$P < 0.05$, $n = 5$ per group per time point. BV/TV, callus bone volume; BMD, bone mineral density; Tb.N, trabecular number; Tb.Th, trabecular thickness; Tb.Sp, trabecular space. (E) Biomechanical testing of the fractured femurs displaying the impaired mechanical property of the new bone in S89G-DMP1 mice at day 28 post-fracture. *$P < 0.05$, $n = 5$ per group per time point.

Impaired chondrogenic and osteogenic differentiation of BMSCs of S89G-DMP1 mice

Given the close association of MSCs and fracture healing, BMSCs were isolated from both groups to assess proliferation, differentiation, and migration. Following the chondrogenic induction for 21 days, Toluidine blue staining was performed to observe the culture aggregates. The BMSCs of the S89G-DMP1 mice displayed lesser staining compared with those of the WT mice (Fig. 5A).

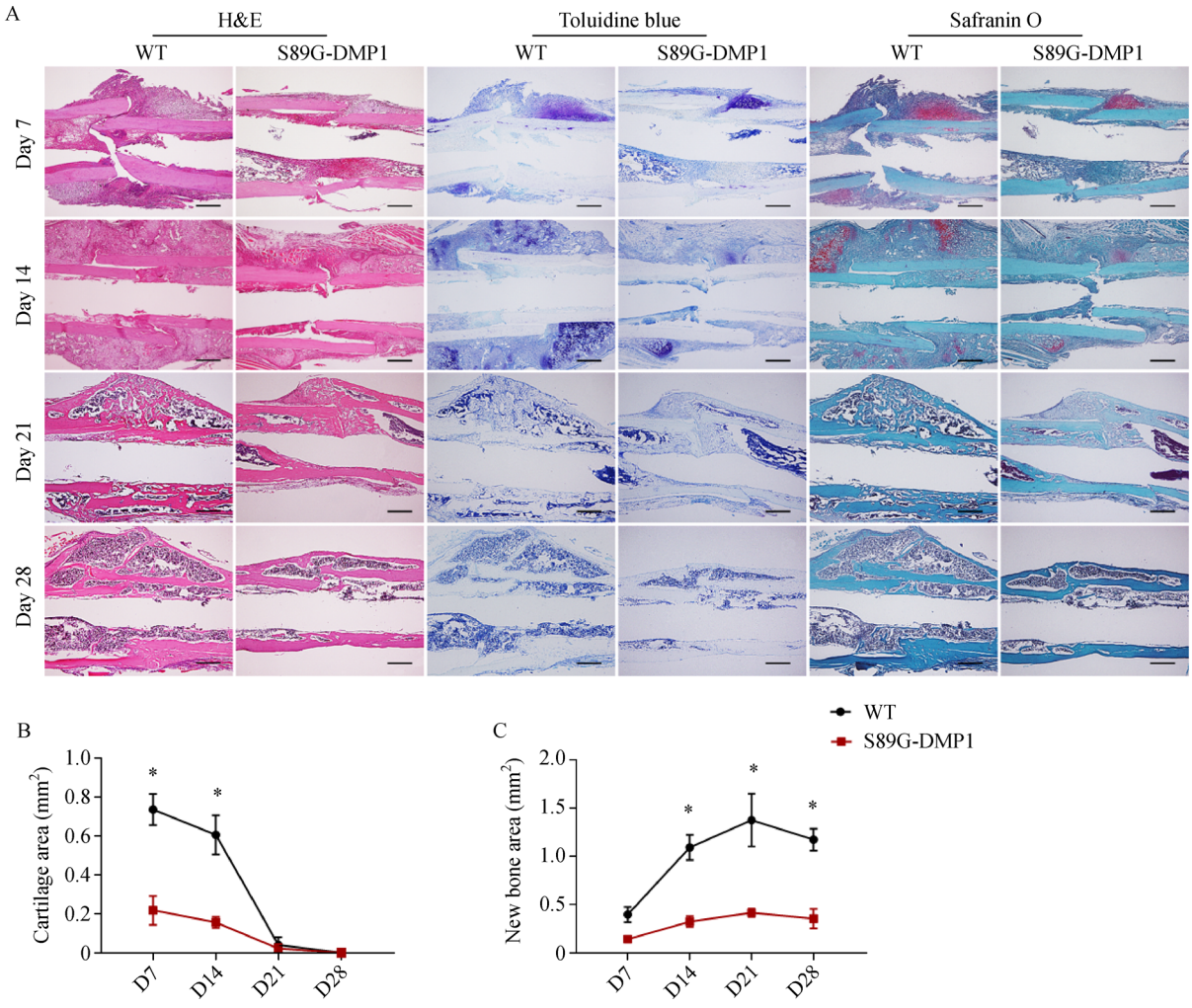

Fig. 3 Histological analysis of the femur fracture healing in WT and S89G-DMP1 mice. (A) H&E, Toluidine blue, and Safranin O staining of fracture calluses showed small cartilaginous calluses and new bone calluses in S89G-DMP1 mice. Scale bars = 500 μm. (B) Quantification of cartilaginous callus areas from (A) is shown as mean ± SEM. $*P < 0.05$, $n = 5$ per group per time point. (C) Quantification of new bone callus areas from (A) is shown as mean ± SEM. $*P < 0.05$, $n = 5$ per group per time point.

After chondrogenic induction, decreased expression levels of chondrogenic marker genes were evident in S89G-DMP1 mice at day 7 (Fig. 5B). CCK-8 assay displayed a weak proliferation capacity of BMSCs from S89G-DMP1 mice at Day 3 but not at other time points (Fig. 5C). In Transwell migration assay, no alteration in cell migration can be detected in either groups (Fig. 5D and 5E).

In addition to the induction of chondrogenesis, osteogenic induction was conducted to detect the discrepancy of bone matrix deposition between the two groups. After 21 days of osteogenic induction, a statistical decrease in matrix deposition was presented by observing the Alizarin red-stained area, which revealed the decreased osteogenic differentiation (Fig. S1A and S1C). The expression levels of osteogenic genes confirmed the impaired differentiation capacity (Fig. S1B). The impaired osteogenic differentiation capacity of BMSCs from S89G-DMP1 mice indicated the potential regulatory role of DMP1-PG in the subsequent woven bone formation at the late stage of fracture healing.

Transcriptome differences in fracture sites between WT and S89G-DMP1 mice

To probe the overall biological functions of DMP1-PG in regulating chondrogenesis within fracture repair, we performed RNA sequencing of the genes from fracture calluses in the S89G-DMP1 and WT mice at day 3 post-fracture. A total of 993 genes showed change, including 382 upregulated genes and 611 downregulated genes

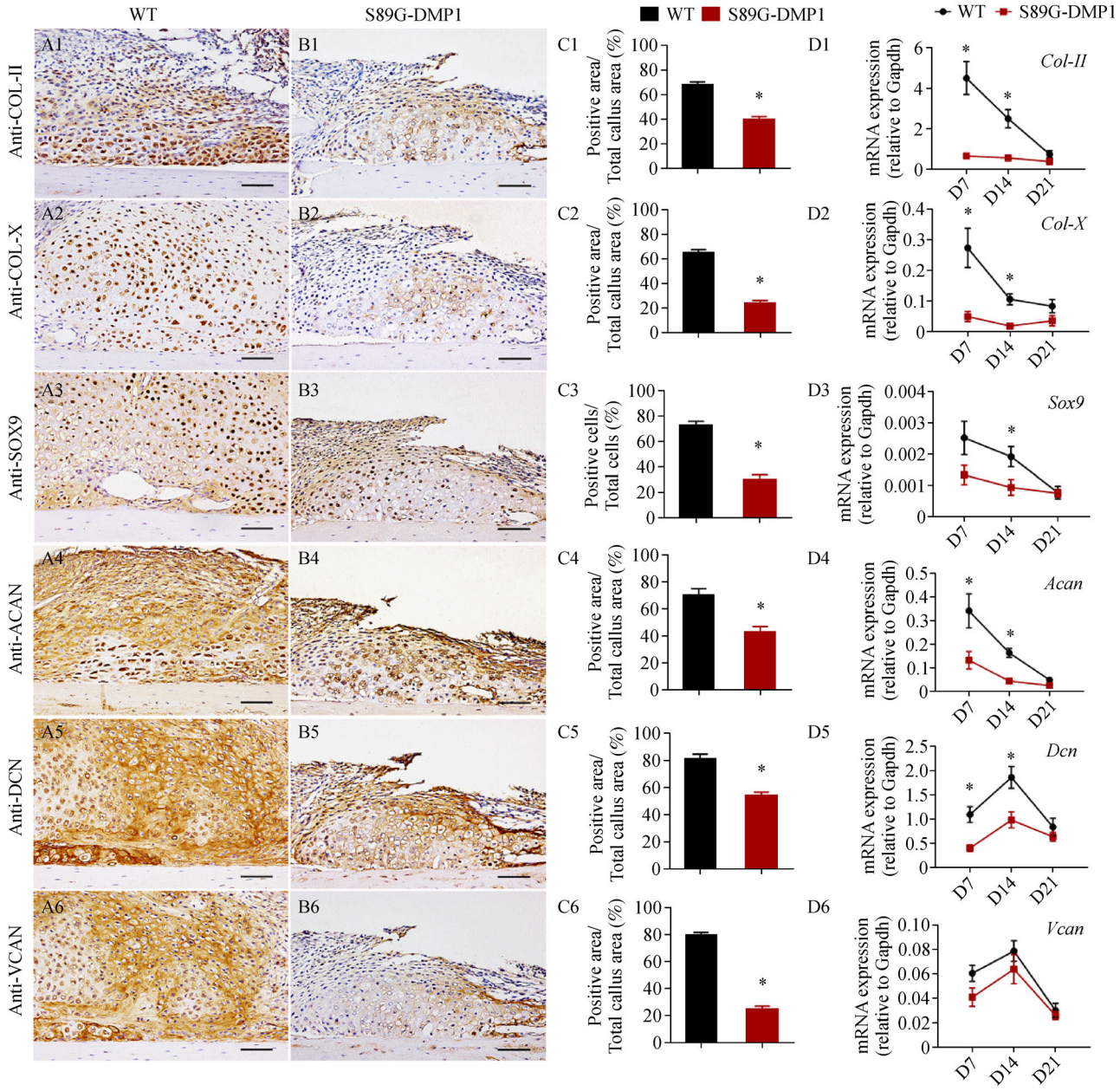

Fig. 4 Alterations of cartilage markers in the cartilaginous calluses of the WT and S89G-DMP1 mice. (A1–A6, B1–B6) Immunohistochemistry staining of COL-II, COL-X, SOX9, ACAN, DCN, and VCAN in cartilaginous callus at day 7 post-fracture. Samples from S89G-DMP1 mice showed remarkably decreased immunoreactivity. Scale bars = 100 μm. (C1–C6) Quantitative measurements of the positive zone area/total callus area or the number of positive cells/number of total cells from the WT and S89G-DMP1 mice are shown as mean ± SEM. *$P < 0.05$, $n = 4$ per group. (D1–D6) RT-qPCR quantification analysis of *Col-II, Col-X, Sox9 Acan, Dcn,* and *Vcan* is presented as mean ± SEM. *$P < 0.05$, $n = 4$–5 per group per time point.

(Fig. 6A and 6B). These altered genes can be categorized into several pathways according to the KEGG analysis (Fig. 6C and 6D). Among these pathways, signaling pathways associated with cell senescence and Janus Kinase/signal transducers and activators of transcription (JAK/STAT) were the top two altered gene pathways.

Changes of IL-6/JAK/STAT signaling in the S89G-DMP1 mice during the fracture healing

RNA sequencing and KEGG analysis showed an impaired JAK/STAT signaling pathway, which indicated that the downregulation of DMP1-PG can affect inflammatory

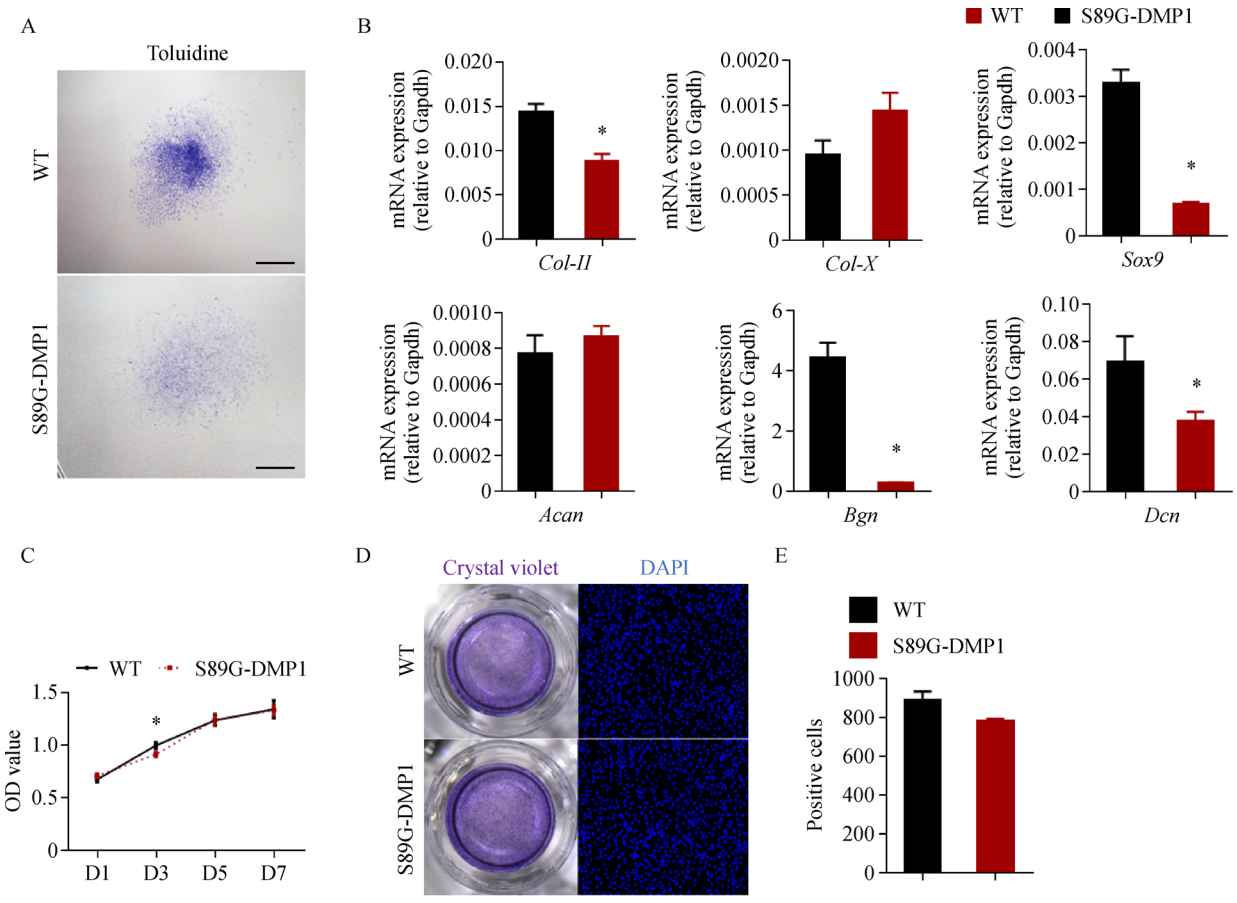

Fig. 5 BMSCs differentiation, proliferation, and migration of WT and S89G-DMP1 mice. (A) Comparison of cultured aggregates from WT and S89G-DMP1 mice is shown by Toluidine blue staining. Scale bars = 1500 μm. (B) The mRNA levels of chondrogenesis-related genes and proteoglycan genes were determined by RT-qPCR. $^*P < 0.05$, $n = 3$ samples per group. (C) A CCK8 assay was performed to analyze the proliferation ability of BMSCs. $^*P < 0.05$, $n = 5$ samples per group. (D) Representative images of Transwell migration assay of BMSCS from the WT group and the S89G-DMP1 group. (E) The quantification of invasive cells of Transwell migration assay is shown as mean ± SEM. $^*P < 0.05$, $n = 4$ samples per group. No difference was found in the ability of migration of BMSCs between the WT and S89G-DMP1 mice.

factors, which in turn disturbed chondrogenesis in fracture repair. Here, we further investigated whether major inflammatory genes related to trauma repair [25], such as *IL-1β*, *IL-6*, *IL-12*, *IL-17,* and *TNF-α*, were involved in PG signaling during fracture healing. The gene expression level of *IL-6* was significantly downregulated in the callus extracts of the S89G-DMP1 mice in contrast to the WT mice at days 1 and 3 post-fracture (Fig. 7A). Immunofluorescence staining confirmed that expression of IL-6 was downregulated in the callus of S89G-DMP1 mice (Fig. 7B). Significantly decreased gene expression levels of *JAK-2* and *STAT-3* were observed, which are core molecules of the JAK/STAT signaling pathway (Fig. 7C). The phosphorylation levels of STAT-3 were downregulated in S89G-DMP1 mice at days 1 and 3 post-fracture based on Western immunoblotting (Fig. 7D). The data presented above indicated that the impaired IL-6/JAK/STAT signaling pathway in the inflammation stage may be one of the mechanisms affecting subsequent chondrogenesis in fracture repair.

Discussion

Although fractures are common and frequently-occurring diseases that endanger human health, the knowledge about fracture healing is still limited. Fracture healing is a well-orchestrated process involving multiple cell types, including MSCs, chondrocytes, osteoblasts, ECM, and signaling molecules, such as components of the Hedgehog signaling pathway [31], BMP/TGF-β signaling pathway, and Wnt /β-catenin signaling pathway [32]. The healing process is also regulated by mechanical environment [33] and chemical factors [34,35]. Following the fracture, under

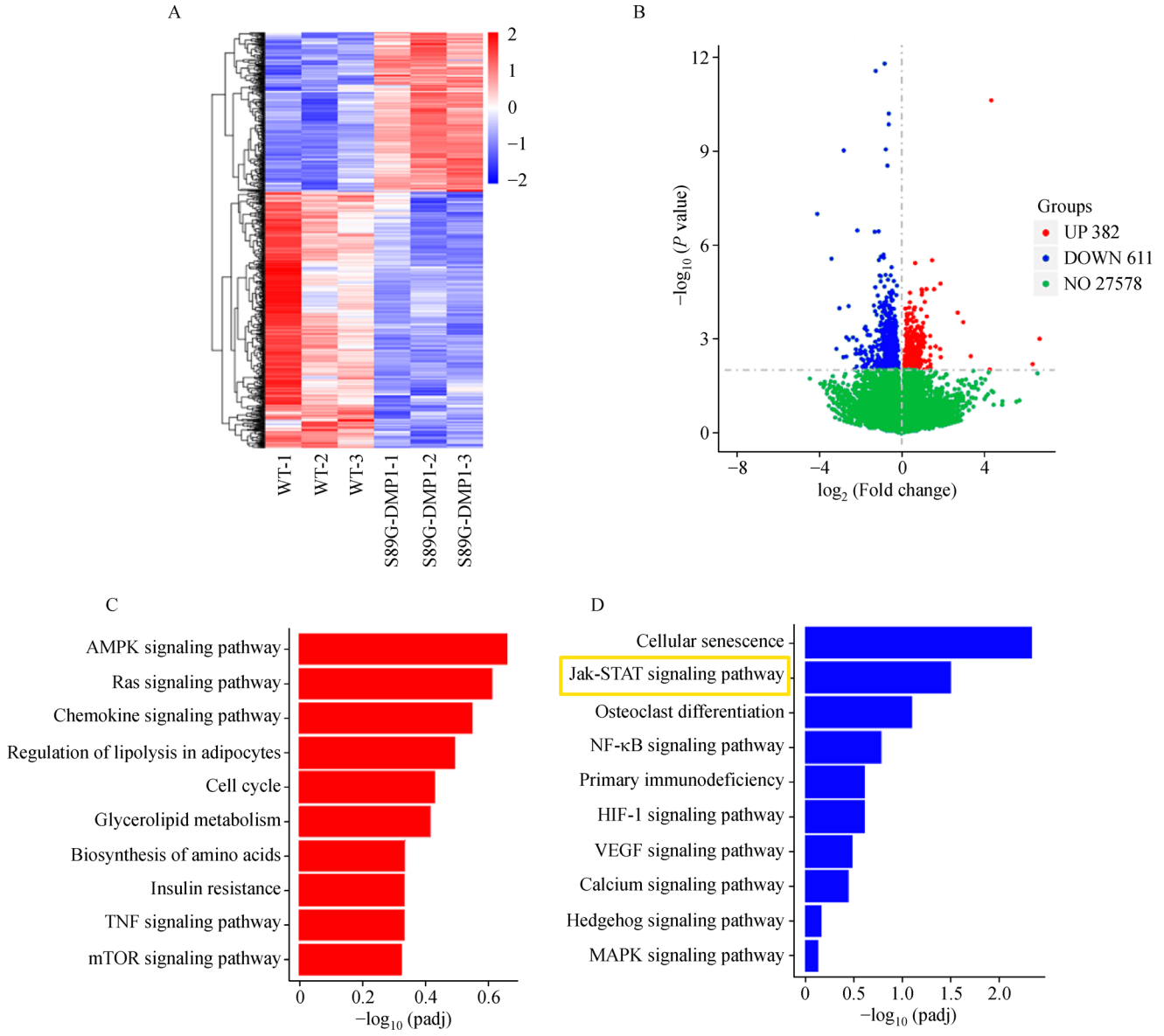

Fig. 6 Differentially expressed mRNA sequences between WT and S89G-DMP1 fracture calluses. (A) Heat map and (B) Volcano plot analysis displayed differentially expressed genes of fracture calluses between the WT and DMP1-S89G mice. KEGG analysis showed the top ten upregulated (C) and downregulated (D) signaling pathways of fracture calluses in S89G-DMP1 mice compared with WT mice.

the stimulation of various signals derived from inflammatory cells, the MSCs surrounding injury sites begin to differentiate into chondrocytes in the central area of fracture gap [3,36,37]. Cartilages are then produced by chondrocytes in the fracture sites to support endochondral bone formation [3,36,38], which can provide mechanical stability with the developing cartilaginous callus [25]. As a key component of cartilage matrix, PGs play crucial roles in cartilage development and maintenance. PGs can condense mesenchyme and modulate the subsequent chondrogenesis [39]. PGs can also interact with collagen and other ECM molecules to maintain the balance of cartilage metabolism. PGs are associated with the degradation of cartilage matrix [9,40], which is critical for the maintenance of cartilage health.

The role of DMP1-PG, a newly identified PG, in articular cartilage development has been studied [9]. Based on this investigation, DMP1-PG was highly expressed in cartilaginous callus after fracture. At day 7 post-fracture, the expression level of DMP1-PG in callus was approximately 50 folds compared with that in the normal bone matrix. However, the loss of DMP1-PG was observed with increased fibrous callus in the aged WT mice at day 7 post-fracture. In the fracture sites of aged mice, the down-

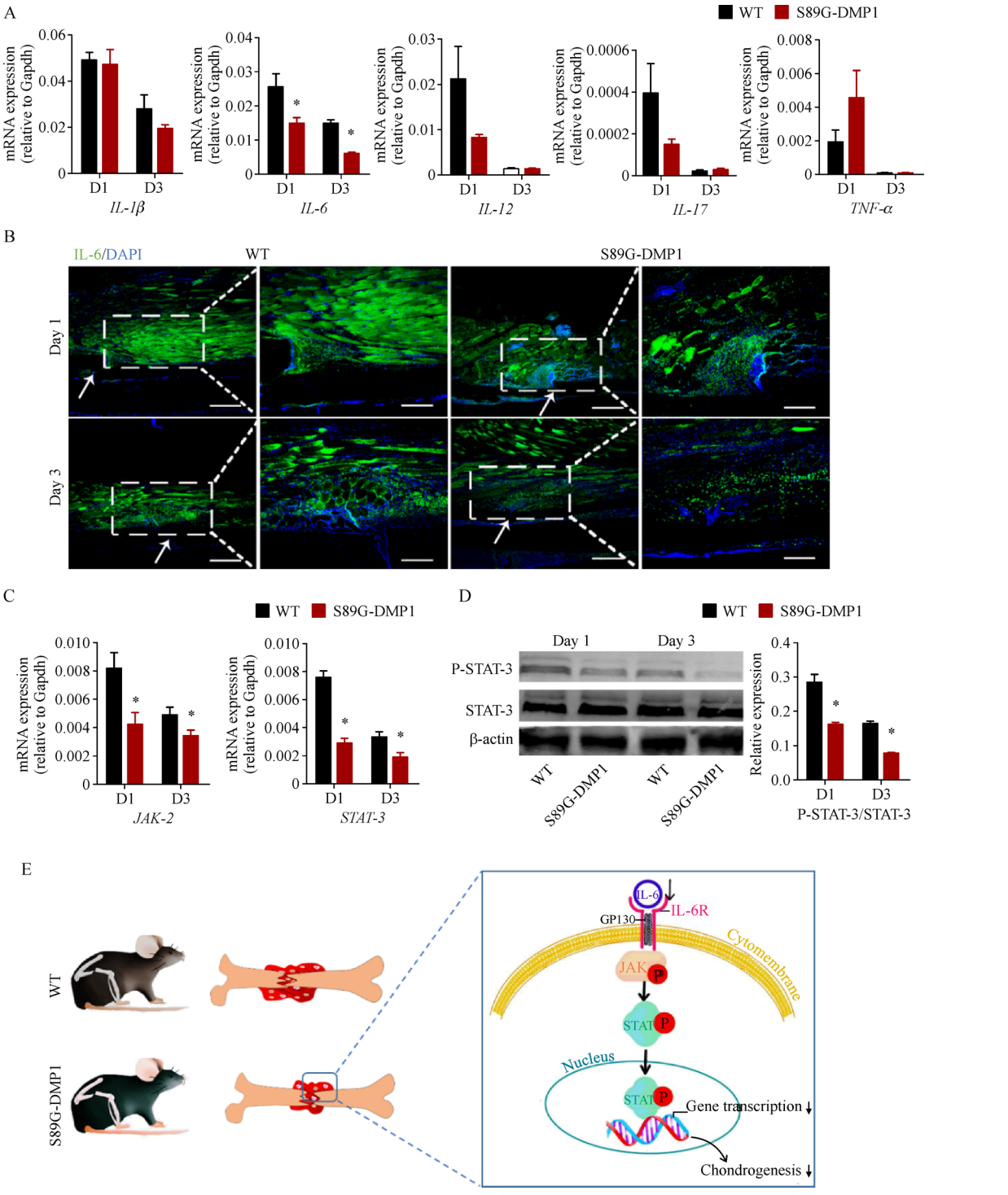

Fig. 7 Detection of IL-6/JAK/STAT signaling in the WT and S89G-DMP1 mice. (A) RT-qPCR quantification of inflammatory molecules during fracture healing is shown as mean ± SEM. *$P < 0.05$, $n = 6$ per group per time point. (B) IL-6 (green) immunofluorescence staining of fracture sites at days 1 and 3 post-fracture. Arrows showed the fracture ends. Lower magnification, scale bars = 500 μm; higher magnification, scale bars = 200 μm. (C) RT-qPCR quantification of JAK/STAT signaling molecules *JAK-2* and *STAT-3* in the fracture calluses at days 1 and 3 post-fracture is shown as mean ± SEM. *$P < 0.05$, $n = 4$ per group per time point. (D) Expression of phosphorylated STAT-3 was downregulated in the fracture site in S89G-DMP1 mice by Western immunoblotting. *$P < 0.05$, $n = 3$ per group per time point. (E) Loss of DMP1-PG affected chondrogenesis in fracture healing.

regulation of DMP1-PG expression and histological morphological changes of callus suggested that DMP1-PG may be an essential molecule in controlling bone fracture repair. Importantly, the expression level of *Dmp1* continued to be upregulated at day 21 post-fracture, whereas the expression levels of other PGs related to cartilage biosynthesis began to decrease. Thus, DMP1-PG may function to modulate both chondrogenesis and the following endochondral ossification.

To further understand the functions of DMP1-PG in regulating cartilaginous callus formation during fracture healing, we employed DMP1 glycosylation site mutation (S89G-DMP1) mice to establish the fracture model. In this model, many types of key PGs are downregulated due to the loss of DMP1-PG [7,9]. In terms of fracture healing, the S89G-DMP1 mice displayed reduced cartilage bridging the fracture sites and delayed endochondral ossification, which resulted in poor fracture healing. In particular, 7 days after the fracture, the gene expression levels of chondrogenesis significantly decreased in the fracture callus of S89G-DMP1 mice. This finding was consistent with the changes detected in Biglycan-deficient mice model during fracture healing [14]. All of these changes indicated that DMP1-PG is a key PG in fracture fusion. The reason why the new bones of S89G-DMP1 mice exhibit weak biomechanical prosperities must also be considered. The decreased PGs can significantly affect osteogenesis in the fracture area [8,41]. Altered PGs affect BMD and strength, which contributes to providing biomechanical properties to withstand loading [42].

To further detect the exact regulatory role of DMP1-PG in cartilage formation during the fracture healing, we conducted transcription analysis. The high-throughput sequencing technique can provide a high coverage of the transcriptome, facilitate the detection of new transcriptome, and allow the investigation of differential gene expression [43]. Clues from RNA sequencing of the fracture callus revealed that JAK/STAT signaling were significantly downregulated in the S89G-DMP1 mice compared with their controls, which indicated that the deficiency of DMP1-PG can affect the expression of inflammation response molecules at the early stage of fracture healing. Based on both RNA sequencing and RT-qPCR analyses, we found that the gene expression level of IL-6 at the injury site decreased significantly in S89G-DMP1 mice at the inflammatory stage. IL-6 is a pleiotropic cytokine produced by a variety of cells and is involved not only in immune events but also in hematopoiesis, tumorigenesis, trauma repairing, stem cell differentiation, and proliferation [44]. IL-6 can bind membrane-anchored receptor (mIL-6R) or soluble receptor, and the association of IL-6/IL-6 receptor with glycoprotein 130 leads to the activation of the JAK/STAT signaling pathway, which regulates cell proliferation, differentiation, and the activities of chondrocytes [45–47]. The release of IL-6 is necessary and critical to initiate injury repair at the early stage of fracture healing [48,49], which is crucial for fracture repair and bone regeneration [50,51]. IL-6 initiates the recruitment of MSCs, stimulates the differentiation of MSCs into chondrocytes and osteoblasts, and promotes angiogenesis [25,52]. In our previous studies, the downstream molecules of IL-6 genes and JAK-2/STAT-3 signaling molecules are markedly affected. The JAK/STAT signaling pathway plays a notable role in the differentiation of various cell types [53]. The crucial role of JAK/STAT signaling pathway in skeletal metabolism and development has been demonstrated using JAK/STAT knockout mice; furthermore, compared with other STAT family members, STAT3 profoundly affects osteoblast differentiation and the transduction of anabolic signals [54]. The alteration of IL-6/STAT-3 signaling can also influence the chondrogenic differentiation of MSCs [54–56].The impairment of the IL-6/JAK-2/STAT-3 signaling affected the binding of STAT3 to target DNA sequences and the following activation of transcription [57]. In the current study, *in vitro* cell culture experiments revealed impaired chondrogenic differentiation ability of BMSCs indicated by decreased cartilage matrix deposition in S89G-DMP1 mice. Based on previous research and the findings of our studies, we speculated that the IL-6/JAK-2/STAT-3 signaling pathway may be involved in cartilage formation during fracture healing, and the downregulation of the IL-6/JAK-2/STAT-3 signaling pathway caused by DMP1-PG deficiency may affect the differentiation of MSCs into chondrocytes and in turn the cartilage-matrix formation, which resulted in the impairment of endochondral ossification and the subsequent bone deposition during fracture healing.

In addition to the altered IL-6/JAK-2/STAT-3 signaling pathway, several other key signaling pathways, such as the cellular senescence pathway, VEGF signaling pathway, and Hedgehog signaling pathway, were downregulated in the S89G-DMP1 mice compared with those of the WT mice during fracture healing. The decreased cellular senescence pathway may trigger MSC influx into the injury sites; however, the weakened differentiation capacity of BMSCs from S89G-DMP1 mice, as evidenced by *in vitro* cell culture experiments, led to the diminished chondrogenesis at the early stage of fracture healing. Increasing reports have demonstrated the positive role of the VEGF signaling pathway in regulating cellular ingress and promoting angiogenesis and bone formation [58,59]. The Hedgehog signaling pathway is also essential for the development of bone and endochondral fracture healing by modulating mesenchymal cell differentiation [36,60]. Thus, DMP1-PG may help maintain several signaling pathways related to trauma repair during healing.

The formation of woven bone is also pivotal at the late

stage of fracture healing. DMP1 is known to exhibit a positive function in bone formation [61]. Based on our previous study, the loss of DMP1-PG can lead to bone loss in both the trabecular bone and cortical bone area [7]. Based on *in vitro* cell culture experiments, we found an impaired osteogenic differentiation capacity of BMSCs from S89G-DMP1 mice. These data indicated that the deficiency of DMP1-PG may also affect bone formation at the late stage of fracture healing.

In summary, our studies support that DMP1-PG can serve as one of the important ECM proteoglycans, which positively regulates the chondrogenesis at the early stage of fracture healing. DMP1-PG deficiency would result in the impairment of cartilaginous callus formation by influencing IL-6/JAK/STAT signaling molecules and injury-related signaling pathways during fracture healing.

Acknowledgements

This study was supported by Key Project of Chinese National Programs for Research and Development (No. 2016YFC1102075, Yao Sun), National Natural Science Foundation of China (Nos. 81470715, 81771043, 81822012, Yao Sun; 81770873, 81722031, Xiaogang Wang; 81670962, Zuolin Wang), Shanghai Health System (No. 2017 BR009, Yao Sun), Tongji University (Nos. TJ15042119036 and TJ2000219143, Zuolin Wang), and Chinese Universities Scientific Fund (No. kx0200020173386, Rui Yue). We would like to appreciate Dr. Chunlin Qin (College of Dentistry, Texas A&M University) for providing the DMP1-N antibody and assistance. We thank Qigang Wang Group, School of Chemical Science and Engineering, Tongji University for providing biomechanical testing machine. We would also like to thank Xiaojuan Yang, Gongchen Li, and Mengmeng Liu for their help in revising the paper.

Compliance with ethics guidelines

Hui Xue, Dike Tao, Yuteng Weng, Qiqi Fan, Shuang Zhou, Ruilin Zhang, Han Zhang, Rui Yue, Xiaogang Wang, Zuolin Wang, and Yao Sun declare no conflict of interest. All institutional and national guidelines for the care and use of laboratory animals were followed.

Electronic Supplementary Material Supplementary material is available in the online version of this article at https://doi.org/10.1007/s11684-019-0693-9 and is accessible for authorized users.

References

1. Schindeler A, McDonald MM, Bokko P, Little DG. Bone remodeling during fracture repair: the cellular picture. Semin Cell Dev Biol 2008; 19(5): 459–466
2. Ai-Aql ZS, Alagl AS, Graves DT, Gerstenfeld LC, Einhorn TA. Molecular mechanisms controlling bone formation during fracture healing and distraction osteogenesis. J Dent Res 2008; 87(2): 107–118
3. Claes L, Recknagel S, Ignatius A. Fracture healing under healthy and inflammatory conditions. Nat Rev Rheumatol 2012; 8(3): 133–143
4. Williams JN, Kambrath AV, Patel RB, Kang KS, Mével E, Li Y, Cheng YH, Pucylowski AJ, Hassert MA, Voor MJ, Kacena MA, Thompson WR, Warden SJ, Burr DB, Allen MR, Robling AG, Sankar U. Inhibition of CaMKK2 enhances fracture healing by stimulating indian hedgehog signaling and accelerating endochondral ossification. J Bone Miner Res 2018; 33(5): 930–944
5. Baht GS, Vi L, Alman BA. The role of the immune cells in fracture healing. Curr Osteoporos Rep 2018; 16(2): 138–145
6. Dimitriou R, Tsiridis E, Giannoudis PV. Current concepts of molecular aspects of bone healing. Injury 2005; 36(12): 1392–1404
7. Sun Y, Weng Y, Zhang C, Liu Y, Kang C, Liu Z, Jing B, Zhang Q, Wang Z. Glycosylation of dentin matrix protein 1 is critical for osteogenesis. Sci Rep 2015; 5(1): 17518
8. Bertassoni LE, Swain MV. The contribution of proteoglycans to the mechanical behavior of mineralized tissues. J Mech Behav Biomed Mater 2014; 38: 91–104
9. Weng Y, Liu Y, Du H, Li L, Jing B, Zhang Q, Wang X, Wang Z, Sun Y. Glycosylation of DMP1 is essential for chondrogenesis of condylar cartilage. J Dent Res 2017; 96(13): 1535–1545
10. Furukawa JI, Okada K, Shinohara Y. Glycomics of human embryonic stem cells and human induced pluripotent stem cells. Glycoconj J 2017; 34(6): 807–815
11. Gao Y, Liu S, Huang J, Guo W, Chen J, Zhang L, Zhao B, Peng J, Wang A, Wang Y, Xu W, Lu S, Yuan M, Guo Q. The ECM-cell interaction of cartilage extracellular matrix on chondrocytes. BioMed Res Int 2014; 2014: 648459
12. Embree MC, Kilts TM, Ono M, Inkson CA, Syed-Picard F, Karsdal MA, Oldberg A, Bi Y, Young MF. Biglycan and fibromodulin have essential roles in regulating chondrogenesis and extracellular matrix turnover in temporomandibular joint osteoarthritis. Am J Pathol 2010; 176(2): 812–826
13. Myren M, Kirby DJ, Noonan ML, Maeda A, Owens RT, Ricard-Blum S, Kram V, Kilts TM, Young MF. Biglycan potentially regulates angiogenesis during fracture repair by altering expression and function of endostatin. Matrix Biol 2016; 52-54: 141–150
14. Berendsen AD, Pinnow EL, Maeda A, Brown AC, McCartney-Francis N, Kram V, Owens RT, Robey PG, Holmbeck K, de Castro LF, Kilts TM, Young MF. Biglycan modulates angiogenesis and bone formation during fracture healing. Matrix Biol 2014; 35: 223–231
15. George A, Sabsay B, Simonian PA, Veis A. Characterization of a novel dentin matrix acidic phosphoprotein. Implications for induction of biomineralization. J Biol Chem 1993; 268(17): 12624–12630
16. D'Souza RN, Cavender A, Sunavala G, Alvarez J, Ohshima T, Kulkarni AB, MacDougall M. Gene expression patterns of murine dentin matrix protein 1 (Dmp1) and dentin sialophosphoprotein (DSPP) suggest distinct developmental functions *in vivo*. J Bone Miner Res 1997; 12(12): 2040–2049
17. Qin C, Brunn JC, Cook RG, Orkiszewski RS, Malone JP, Veis A, Butler WT. Evidence for the proteolytic processing of dentin matrix

protein 1. Identification and characterization of processed fragments and cleavage sites. J Biol Chem 2003; 278(36): 34700–34708
18. Qin C, D'Souza R, Feng JQ. Dentin matrix protein 1 (DMP1): new and important roles for biomineralization and phosphate homeostasis. J Dent Res 2007; 86(12): 1134–1141
19. Lu Y, Yuan B, Qin C, Cao Z, Xie Y, Dallas SL, McKee MD, Drezner MK, Bonewald LF, Feng JQ. The biological function of DMP-1 in osteocyte maturation is mediated by its 57-kDa C-terminal fragment. J Bone Miner Res 2011; 26(2): 331–340
20. Lu Y, Qin C, Xie Y, Bonewald LF, Feng JQ. Studies of the DMP1 57-kDa functional domain both *in vivo* and *in vitro*. Cells Tissues Organs 2009; 189(1-4): 175–185
21. Sun Y, Ma S, Zhou J, Yamoah AK, Feng JQ, Hinton RJ, Qin C. Distribution of small integrin-binding ligand, N-linked glycoproteins (SIBLING) in the articular cartilage of the rat femoral head. J Histochem Cytochem 2010; 58(11): 1033–1043
22. Sun Y, Chen L, Ma S, Zhou J, Zhang H, Feng JQ, Qin C. Roles of DMP1 processing in osteogenesis, dentinogenesis and chondrogenesis. Cells Tissues Organs 2011; 194(2-4): 199–204
23. Qin C, Huang B, Wygant JN, McIntyre BW, McDonald CH, Cook RG, Butler WT. A chondroitin sulfate chain attached to the bone dentin matrix protein 1 NH_2-terminal fragment. J Biol Chem 2006; 281(12): 8034–8040
24. Gericke A, Qin C, Sun Y, Redfern R, Redfern D, Fujimoto Y, Taleb H, Butler WT, Boskey AL. Different forms of DMP1 play distinct roles in mineralization. J Dent Res 2010; 89(4): 355–359
25. Loi F, Córdova LA, Pajarinen J, Lin TH, Yao Z, Goodman SB. Inflammation, fracture and bone repair. Bone 2016; 86: 119–130
26. Bradaschia-Correa V, Josephson AM, Mehta D, Mizrahi M, Neibart SS, Liu C, Kennedy OD, Castillo AB, Egol KA, Leucht P. The selective serotonin reuptake inhibitor fluoxetine directly inhibits osteoblast differentiation and mineralization during fracture healing in mice. J Bone Miner Res 2017; 32(4): 821–833
27. Baht GS, Nadesan P, Silkstone D, Alman BA. Pharmacologically targeting β-catenin for NF1 associated deficiencies in fracture repair. Bone 2017; 98: 31–36
28. Balic A, Aguila HL, Caimano MJ, Francone VP, Mina M. Characterization of stem and progenitor cells in the dental pulp of erupted and unerupted murine molars. Bone 2010; 46(6): 1639–1651
29. Jing B, Zhang C, Liu X, Zhou L, Liu J, Yao Y, Yu J, Weng Y, Pan M, Liu J, Wang Z, Sun Y, Sun YE. Glycosylation of dentin matrix protein 1 is a novel key element for astrocyte maturation and BBB integrity. Protein Cell 2018; 9(3): 298–309
30. Wang C, Abu-Amer Y, O'Keefe RJ, Shen J. Loss of Dnmt3b in chondrocytes leads to delayed endochondral ossification and fracture repair. J Bone Miner Res 2018; 33(2): 283–297
31. Baht GS, Silkstone D, Nadesan P, Whetstone H, Alman BA. Activation of hedgehog signaling during fracture repair enhances osteoblastic-dependent matrix formation. J Orthop Res 2014; 32(4): 581–586
32. Majidinia M, Sadeghpour A and Yousefi B. The roles of signaling pathways in bone repair and regeneration. J Cell Physiol 2018; 233 (4): 2937–2948
33. Ghiasi MS, Chen J, Vaziri A, Rodriguez EK, Nazarian A. Bone fracture healing in mechanobiological modeling: a review of principles and methods. Bone Rep 2017; 6: 87–100
34. Klontzas ME, Kenanidis EI, MacFarlane RJ, Michail T, Potoupnis ME, Heliotis M, Mantalaris A, Tsiridis E. Investigational drugs for fracture healing: preclinical & clinical data. Expert Opin Investig Drugs 2016; 25(5): 585–596
35. Richards CJ, Graf KW Jr, Mashru RP. The effect of opioids, alcohol, and nonsteroidal anti-inflammatory drugs on fracture union. Orthop Clin North Am 2017; 48(4): 433–443
36. Gerstenfeld LC, Cullinane DM, Barnes GL, Graves DT, Einhorn TA. Fracture healing as a post-natal developmental process: molecular, spatial, and temporal aspects of its regulation. J Cell Biochem 2003; 88(5): 873–884
37. Tsiridis E, Upadhyay N, Giannoudis P. Molecular aspects of fracture healing: which are the important molecules? Injury 2007; 38(Suppl 1): S11–S25
38. Hsu WK, Anderson PA. Odontoid fractures: update on management. J Am Acad Orthop Surg 2010; 18(7): 383–394
39. Williams DR Jr, Presar AR, Richmond AT, Mjaatvedt CH, Hoffman S, Capehart AA. Limb chondrogenesis is compromised in the versican deficient hdf mouse. Biochem Biophys Res Commun 2005; 334(3): 960–966
40. Lord MS, Farrugia BL, Rnjak-Kovacina J, Whitelock JM. Current serological possibilities for the diagnosis of arthritis with special focus on proteins and proteoglycans from the extracellular matrix. Expert Rev Mol Diagn 2015; 15(1): 77–95
41. Nikitovic D, Aggelidakis J, Young MF, Iozzo RV, Karamanos NK, Tzanakakis GN. The biology of small leucine-rich proteoglycans in bone pathophysiology. J Biol Chem 2012; 287(41): 33926–33933
42. Li S, Cao J, Caterson B, Hughes CE. Proteoglycan metabolism, cell death and Kashin-Beck disease. Glycoconj J 2012; 29(5-6): 241–248
43. Kukurba KR, Montgomery SB. RNA sequencing and analysis. Cold Spring Harb Protoc 2015; 2015(11): 951–969
44. Naka T, Nishimoto N, Kishimoto T. The paradigm of IL-6: from basic science to medicine. Arthritis Res 2002; 4(Suppl 3): S233–S242
45. O'Shea JJ, Schwartz DM, Villarino AV, Gadina M, McInnes IB, Laurence A. The JAK-STAT pathway: impact on human disease and therapeutic intervention. Annu Rev Med 2015; 66(1): 311–328
46. Liongue C, Sertori R, Ward AC. Evolution of cytokine receptor signaling. J Immunol 2016;197(1):11–18
47. Beier F, Loeser RF. Biology and pathology of Rho GTPase, PI-3 kinase-Akt, and MAP kinase signaling pathways in chondrocytes. J Cell Biochem 2010; 110(3): 573–580
48. Fazzalari NL. Bone fracture and bone fracture repair. Osteoporos Int 2011; 22(6): 2003–2006
49. Sun G, Wang Z, Ti Y, Wang Y, Wang J, Zhao J, Qian H. STAT3 promotes bone fracture healing by enhancing the FOXP3 expression and the suppressive function of regulatory T cells. APMIS 2017; 125(8): 752–760
50. Mountziaris PM, Spicer PP, Kasper FK, Mikos AG. Harnessing and modulating inflammation in strategies for bone regeneration. Tissue Eng Part B Rev 2011; 17(6): 393–402
51. Osta B, Benedetti G, Miossec P. Classical and paradoxical effects of TNF-α on bone homeostasis. Front Immunol 2014; 5: 48
52. Wu AC, Raggatt LJ, Alexander KA, Pettit AR. Unraveling macrophage contributions to bone repair. Bonekey Rep 2013; 2: 373
53. Jang YN, Baik EJ. JAK-STAT pathway and myogenic differentia-

tion. JAK-STAT 2013; 2(2): e23282

54. Li J. JAK-STAT and bone metabolism. JAK-STAT 2013; 2(3): e23930
55. Kondo M, Yamaoka K, Sakata K, Sonomoto K, Lin L, Nakano K, Tanaka Y. Contribution of the interleukin-6/STAT-3 signaling pathway to chondrogenic differentiation of human mesenchymal stem cells. Arthritis Rheumatol 2015; 67(5): 1250–1260
56. Pass C, MacRae VE, Huesa C, Faisal Ahmed S, Farquharson C. SOCS2 is the critical regulator of GH action in murine growth plate chondrogenesis. J Bone Miner Res 2012; 27(5): 1055–1066
57. Kim H, Sonn JK. Rac1 promotes chondrogenesis by regulating STAT3 signaling pathway. Cell Biol Int 2016; 40(9): 976–983
58. Hankenson KD, Dishowitz M, Gray C, Schenker M. Angiogenesis in bone regeneration. Injury 2011; 42(6): 556–561
59. Hankenson KD, Gagne K, Shaughnessy M. Extracellular signaling molecules to promote fracture healing and bone regeneration. Adv Drug Deliv Rev 2015; 94: 3–12
60. Alman BA. The role of hedgehog signalling in skeletal health and disease. Nat Rev Rheumatol 2015; 11(9): 552–560
61. Feng JQ, Ward LM, Liu S, Lu Y, Xie Y, Yuan B, Yu X, Rauch F, Davis SI, Zhang S, Rios H, Drezner MK, Quarles LD, Bonewald LF, White KE. Loss of DMP1 causes rickets and osteomalacia and identifies a role for osteocytes in mineral metabolism. Nat Genet 2006; 38(11): 1310–1315